UNIVERSITY OF NORTH CAROLINA AT CHAPEL HILL

DEPARTMENT OR COMPUTER SCIENCE

SENIOR HONORS THESIS

A frameless image sensor with application in astronomy

By

Yi HU

Advisor:
Montek SINGH

Second Reader:
Ketan MAYER-PATEL

September 24, 2024

Abstract

In this thesis, we reviewed the basics of image sensors and compared the conventional CCD and CMOS image sensors with a frameless imaging design. With a focus on application in astronomy, we developed three methods that reduce the noise floor of the frameless sensor to improve its performance under low-light environment typical in astronomy, and introduced single photon detection for extreme dark environment.

Acknowledgements

I would like to thank my thesis advisor Professor Montek Singh of the Computer Science Department at the University of North Carolina. He patiently guided me throughout my studies and taught me how to defend my thesis. He consistently allowed this paper to be my own work, but steered me in the right the direction whenever he thought I needed it.

Contents

List of Figures

List of Tables

List of Symbols

D	dark current	A/pixel (electrons/pixel/s)
T	temperature	K
t	time	s
N_r	read noise per pixel	electrons rms/pixel
P	incident photon flux per pixel	photons/pixel/s
B	background photon flux per pixel	photons/pixel/s
Q_e	quantum efficiency	%
$\mathcal{R}$	surface reflectance	%
N_{sat}	full well capacity per pixel	electrons/pixel
E_{ph}	photon energy	J
E_g	bandgap	J
E_C	conduction band energy	J
E_V	valence band energy	J
ν	photon frequency	s^{-1}
I_{ph}	photocurrent	A
t_{int}	integration time	s
V_0	built-in potential of diodes	V
V_{BD}	breakdown voltage of the SPAD	V
V_{EX}	excessive voltage of the SPAD	V
v_g	gate voltage	V
λ	wavelength	m
η	quantum frequency at certain depth	%
α	absorption coefficient	

List of Abbreviations

CCD	**C**harge-**C**oupled **D**evice
CMOS	**C**omplementary **M**etal-**O**xide-**S**emicondector
MOS	**M**etal-**O**xide-**S**emicondector
SPAD	**S**ingle-**P**hoton **A**valanche **D**iode
SNR	**S**ignal-to-**N**oise **R**atio
DR	**D**ynamic **R**ange
FF	**F**ill **F**actor
QE	**Q**uantum **E**fficiency
PPD	**P**inned **P**hoto**d**iodes
FD	**F**loating **D**iffusion
DCR	**D**ark **C**ount **R**ate
PDP	**P**hoton **D**etection **P**robability
PPS	**P**assive **P**ixel **S**ensor
APS	**A**ctive **P**ixel **S**ensor

Chapter 1

Introduction

1.1 Motivation and Research Objectives

1.1.1 Motivation

Since the dawn of photography in the early 19th century, camera design has continued to evolve around the same idea: a shutter opens, the camera collects and records the incoming light and then, after a certain period of time, the shutter closes to end the light capture. Traditionally, this recording was performed using photographic film, but the modern era has seen film replaced by electronic image sensors. But despite the remarkably different medium, the central idea has remained the same: the entire area is illuminated using a shutter for a fixed time interval. This forced synchronicity — i.e., all pixels must be activated and deactivated at the same time — is unnecessary and has severe drawbacks: the dynamic range, precision, and sensitivity of the camera are limited.

It is true that fixing the time frames simplify the sensor design, but all the constraints will keep existing if the sensor architecture keeps relying heavily on framed capture. A new approach, instead of measuring light in discrete time intervals, is to record the time each pixel takes to accumulate a certain number of photons. Once the number has been met, a “tick" event is triggered. As a result, the frequency of a pixel triggering “tick" events will be proportional to the light intensity at that spot. Pixels of higher intensity will trigger “tick" events much frequently than those of lower light intensity. This change from counting photons over a fixed time interval, to measuring time for a fixed number of photons will overcome barriers and limitations of previous methods by allowing frameless, asynchronous stream of high dynamic range pixel data.

1.1.2 Research Objectives

The goal of this research is to build upon an existing asynchronous frameless camera architecture design and make feasible its application for general photography and astronomy. The physics of basic electronics and conventional image sensors (CCD and CMOS) will be reviewed and compared with the new asynchronous image sensor for a complete evaluation.

We also propose two improvements for the new sensor design: one that increases the low-light detection by reducing the noise; the other enables

single photon detection by implementing single-photon avalanche diodes (SPADs). Both of them give the new frameless sensor architecture greater application power for the use in general photography and astrophotography.

1.2 Domain Requirements

1.2.1 General Purpose Photography

For general purpose photography, some of the most important sensor considerations pertinent to our project are:

Camera Resolution: the amount of detail that the camera can capture is called the resolution, and it is measured in pixels. The more pixels a camera has, the more detail it can capture and the larger pictures can be without becoming blurry.

Dynamic Range: defined to be the maximum signal divided by the noise floor in a pixel. It reflects the ability of the sensor to more evenly capture the bright and shadow areas of an image and is increased with greater pixel sizes.

Light Sensitivity: describes how sensitive each pixel responds to a change in light intensity. It is determined by quantum efficiency, pixel size and noise characteristics.

Frame Rate: the measure of how many times the full pixel array can be read in a second. It depends on the sensor readout speed, the data transfer rate of the interface including cabling, and the number of pixels (amount of data transferred per frame).

Mentioned above are main factors that are critical for the performance of general cameras. Some of them are especially important to cameras for specific use. For example, frame rate is key to high speed camera.

1.2.2 Astronomy

In the field of astronomy, some of the requirements for the camera sensor are more rigid than for general purpose photography because of the specialty of the subjects. In addition, there are also other factors to consider.

High Resolution: a must to discern every single tiny star in space.

Low-light Sensitivity: because the targets are often very faint, high sensitivity under low-light environment is required for the camera to operate properly.

Signal-to-Noise Ratio (SNR): the ratio of the signal to the noise. It has to be high under low-light environment.

Dynamic Range: because bright and faint stars are often captured in a single photo, high dynamic range is required for astrophotography.

In general, frame rate is not considered for astronomy not only because the subjects are relatively static, but also because exposure is longer for astrophotography in order to collect enough photons.

1.3 Organization of the Thesis

This thesis is divided into three parts: Chapter 2 and Chapter 3 form the first part that introduces the technological background for this work, Chapter 4 and Chapter 5 talk about my contribution to the existing asynchronous image sensor design, and Chapter 6 concludes the project.

Specifically, Chapter 2 gives the performance metrics to evaluate camera sensor, and a general overview of the sensor technologies with a special focus on conventional CCD and CMOS sensors. Chapter 3 introduces the asynchronous frameless imaging sensor design that my research is built upon. My two contributions to the design is explained in detail in Chapter 4 and 5. The first improvement is in the low-light detection of the sensor and is achieved by noise reduction – specifically the reset noise – through two-threshold sampling and accelerated sampling via current injection. The second improvement is to enable single photon detection by implementing SPADs in pixel circuitry. Chapter 6 summarizes the project and evaluates the two improvements by comparing them with conventional CCD and CMOS sensors. A discussion of future work is also included.

Chapter 2

Background: Sensors

2.1 Introduction: Conventional CCD and CMOS Sensors

CMOS (Complementary Metal-Oxide-Semiconductor) and CCD (Charge-Coupled Device) are most common types of sensors used in digital imaging. They have similar components, but different readout "circuitries." In CCDs, charge is shifted out, while in CMOS sensors, charge or voltage is read out using row and column decoders.

The basics of frame-transfer CCD architecture is shown in Fig.2.1. After the photodetectors collect photons, the photon-generated charges are first shifted to the vertical analog shift registers. Then, with the whole frame moving downward, the bottom row is shifted to the bottom horizontal CCDs. Finally, the horizontal CCDs move horizontally and output each pixel of the row one by one through the output amplifier. Such serial readout is repeated until all the pixels of each row are read.

Unlike CCDs, the CMOS architecture shown in Fig.2.2 has an amplifier integrated inside each pixel unit so that the information on each pixel can be immediately accessed and read through the outside circuitry. Such arrangement significantly increases the readout speed and makes CMOS a more promising choice for future sensor generations.

In general, CCDs are preferred in astrophotography because they have high signal-to-noise performance under low-light conditions that allows them to be more accurate over long-exposure shots, and a more uniform readout across all pixels than CMOS devices. But CMOS sensors are much more efficient in energy and in processing speed than CCDs. More detailed explanation and comparison are given in Section 2.4.

2.2 Performance Metrics for Image Sensors

- **Signal-to-Noise Ratio (SNR)**: the ratio of the total signal (true signal plus the noise) to the noise alone.
- **Dynamic Range (DR)**: the ratio of the maximum signal to the noise floor in a pixel.

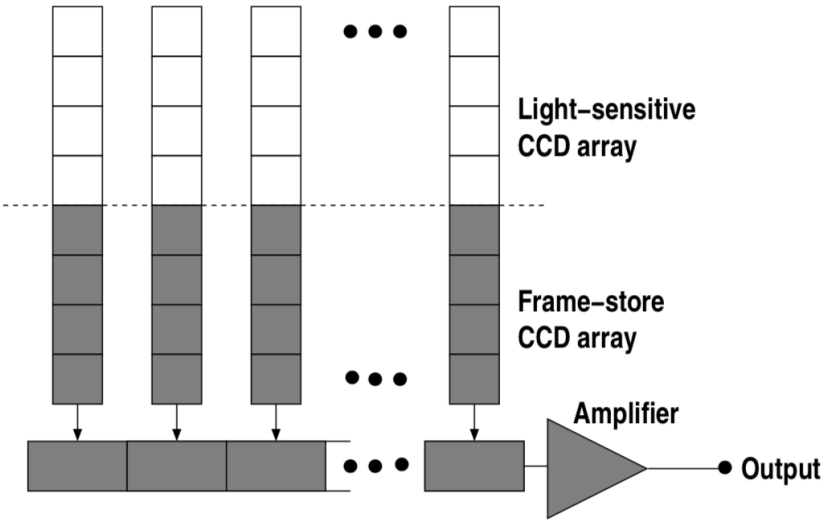

FIGURE 2.1: Simplified frame-transfer(FT) CCD architecture. (Source: [4])

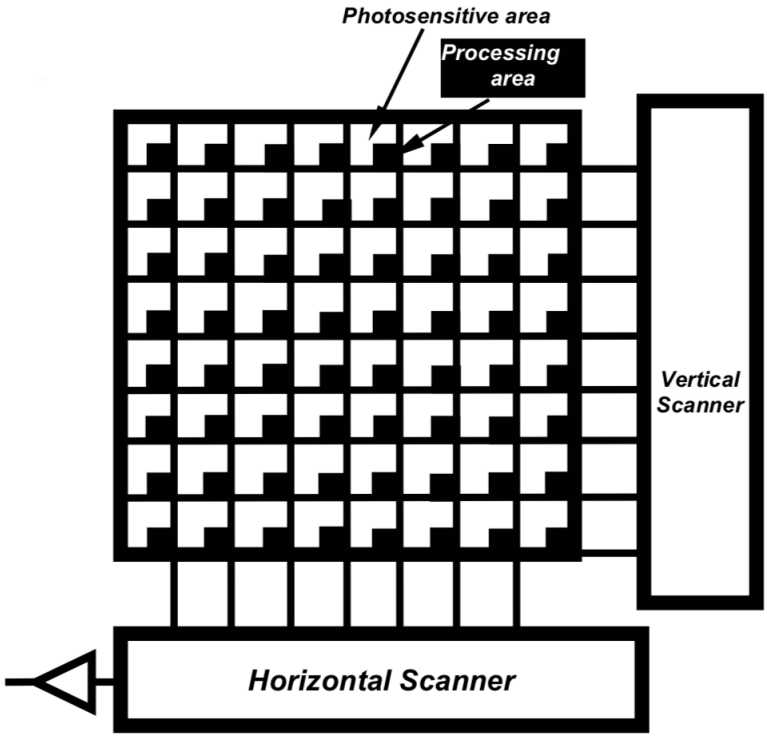

FIGURE 2.2: Simplified CMOS architecture. (Source: [11])

- **Frame Rate**: the number of times the whole picture frame can be read in one second.
- **Dark Current**: the rate of generation of thermal electrons at a given temperature.
- **Fill Factor (FF)**: the ratio of a pixel's light sensitive area to its total area.
- **Quantum Efficiency (QE)**: the ratio of the charge created by the device for a specific number of incoming photons at a given wavelength.
- **Cost and Power Consumption**: the cost of production and the power consumption during operation.

2.2.1 Signal-to-Noise Ratio (SNR)

The signal-to-noise ratio (SNR) for a camera represents the ratio of the measured light signal to the combined noise that includes three primary sources: photon noise, dark noise, and read noise.

1. **Photon Noise**: the inherent statistical variation in the number of incident photons that cannot be reduced. Since the interval between photon arrivals follows Poisson statistics, Photon Noise $= \sqrt{\#\text{incident photons}}$.
2. **Dark Noise**: the statistical variation in the number of thermally generated electrons within the silicon. Like photon noise, it also exhibits a Poisson distribution, and Dark Noise $= \sqrt{\#\text{thermal electrons}} = \sqrt{D(T) \cdot t}$ where $D(T)$ (electrons/pixel/second) denotes the dark current at a given temperature T and t (seconds) is the integration time.
3. **Read Noise**: the collective electronic noise sources inherent to the camera system and the sensor. We denote the read noise root-mean-square (rms) by N_r.

With the three primary components of noise considered, SNR can be calculated as follows[5]:

$$SNR = \frac{PQ_e t}{\sqrt{(P+B)Q_e t + D(T) \cdot t + N_r^2}} \tag{2.1}$$

where P is the incident photon flux (photons/pixel/second), B is the unwanted background photon flux (photons/pixel/second), Q_e is the quantum efficiency which will be talked about in Section 2.2.6, $D(T)$ is the dark current (electrons/pixel/second) at a given temperature T, t is the integration time (seconds), and N_r is the read noise (electrons rms/pixel).

2.2.2 Dynamic Range (DR)

The dynamic range reflects how evenly the camera can capture the bright and shadow areas of an image and is defined to be the ratio of the maximum achievable signal to the minimum discernible signal in a pixel. The

maximum signal is determined by the full well capacity per pixel, which is proportional to the size of the individual photodiode, while the minimum discernible signal is limited by the noise floor. So the dynamic range can be calculated following[5]:

$$\text{Dynamic Range per pixel} = \frac{\text{Full Well Capacity per pixel(electrons)}}{\text{Noise Floor per pixel(electrons)}}. \quad (2.2)$$

The noise floor is governed by the read noise. Therefore, Noise Floor per pixel(electrons) = N_r. If we use N_{sat} (electrons) express the full well capacity per pixel, the DR per pixel is expressed as:

$$\text{DR per pixel} = \frac{N_{sat}}{N_r}. \quad (2.3)$$

Alternatively, the DR is expressed in decibel units according to the following equation:

$$\text{DR per pixel (dB)} = 20 \times \log\left(\frac{N_{sat}}{N_r}\right). \quad (2.4)$$

2.2.3 Frame Rate

The frame rate of a camera system is a factor crucial to the ability of the system to record data at high frequency. It is determined by the combined frame acquisition time and frame read time, which depend on the camera system and the kind of application. Therefore, quantitatively[6]

$$\text{Frame Rate (fps)} = \frac{1}{\text{Frame Acquisition Time} + \text{Frame Read Time}}. \quad (2.5)$$

2.2.4 Dark Current

The dark current is the current generated by thermal effect without incident photons. It depends significantly on the temperature so is denoted as a function of temperature $D(T)$. As with photon noise, the noise from the dark current is the square root of the number of thermal generated electrons. At temperature T with integration time t, we can calculate the dark noise from the dark current $D(T)$ as follows[3]:

$$\text{Dark Noise (electrons/pixel)} = \sqrt{D(T) \cdot t}. \quad (2.6)$$

2.2.5 Fill Factor (FF)

Fill factor (FF) is a highly used metric in terms of pixel layout. It is the ratio of the photo-collection area to the total pixel area and is often listed as a percentage.

$$FF = \frac{\text{Photocollection area}}{\text{Pixel area}}. \quad (2.7)$$

2.2.6 Quantum Efficiency (QE)

Quantum efficiency (QE) measures how effective the camera produces electrons from incident photons and is defined as the probability that an incident photon will generate an electron-hole pair that will contribute to the detection signal. If we denote QE for a particular wavelength λ at certain depth d into the material by $\eta(d)$, it can be expressed as[13]:

$$\eta(d) = (1 - \mathcal{R})\zeta(1 - e^{-\alpha d}) \tag{2.8}$$

where $\mathcal{R}$ is the surface reflectance, ζ is the probability that the generated electron-hole pair will contribute to the detected signal and α is the absorption coefficient of the material for wavelength λ. QE can be calculated by integrating $\eta(d)$ from 0 to the thickness of the material. It is a function of wavelength, and is measured as a percentage. If we denote QE at wavelength λ by $Q_e(\lambda)$, and $P(\lambda)$ is the photon influx for the particular wavelength λ, the number of generated electrons in the sensor within integration time t can be calculated as follows:

$$\text{\#photo-generated electrons} = t \cdot \int_0^\infty Q_e(\lambda)P(\lambda)d\lambda. \tag{2.9}$$

QE is a factor crucial to the light sensitivity of the sensor, and also determines the sensor performance under low-light environment. 95% QE means that for 100 incoming photons, around 95 electrons are generated.

2.2.7 Cost and Power Consumption

The cost of production of the sensor depends on how specialized and complicated the manufacturing process is. CMOS image sensors are cheaper because they can be produced by standard CMOS manufacturing process, while CCD sensors are more expensive because they require a more specialized process.

Power consumption is another important metric. It is generally proportional to the square of the supply voltage and the clocking frequency. Some design trade-offs need to be considered. While we can reduce the power consumption by decreasing the supply voltage, the voltage range for digitization is also decreased. Also, we can reduced the power consumption by limiting the frequency, at the expense of a lowered frame rate.

2.3 Physics of Photodetectors

Photodetectors form the front end of an image sensor and their characteristics directly influence the performance of the entire imager system. Ideally, they produce photo-current proportional to the intensity of the incident light.

Semiconductor like silicon has an energy gap between its valence band and the conduction band, which is called the bandgap and is denoted by E_g.

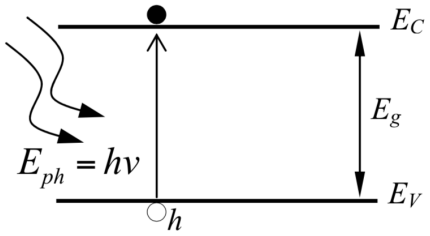

FIGURE 2.3: Electron-hole generation by excitation with photons of energy $E_{ph} > E_g$. (Source: [11])

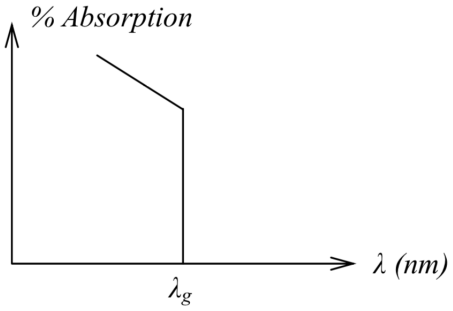

FIGURE 2.4: Absorption spectrum (Source: [11])

When hit by a photon whose energy is greater than the bandgap, the semiconductor will absorb the photon and produce an electron-hole pair with a probability equal to QE at that wavelength. This generation of free electron-hole pairs is referred to as photoelectric effect. Note that for a photon, its energy $E_{ph} = h\nu = hc/\lambda$, where h is the Plank's constant, ν is the light frequency, c is the speed of light and $\lambda = c/\nu$ is the photon's wavelength.

Fig.2.3 shows the generation of a electron-hole pair with a photon of energy $E_{ph} > E_g$. Since only photons whose energies satisfy $E_{ph} > E_g$ can generate electron-hole pairs, the absorption spectrum shown in Fig.2.4 has a sharp edge at $\lambda_g = E_g/hc$, beyond which point the absorption is zero.

Photodetectors are devices that exploit the photoelectric effect to convert the photon influx to photocurrent. The following subsections will introduce some of the most common devices used in the sensor chips that are also related to this project.

2.3.1 Photodiodes

Photodiode is one of the most frequently used photodetectors. They are semiconductor devices which contain a PN junction, or a PN junction with an intrinsic (undoped) layer between N and P layers. The latter are called P–i–N or PIN photodiodes.

Fig.2.5 gives an ideal model of a PN junction without external electric field, where N_a is the acceptor density, N_d is the donor density, W is the depletion width, E_f is the Fermi energy, E_v is the top of the valance band and E_c is the bottom of the conduction band. Fig.2.5(a) gives the structure of a PN junction, Fig.2.5(b) the resulting electron and hole density distribution,

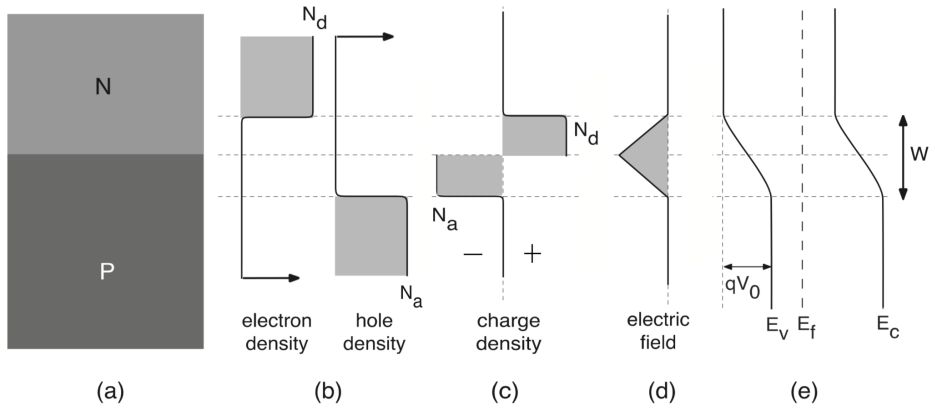

FIGURE 2.5: Ideal PN junction properties. (Source: [13])

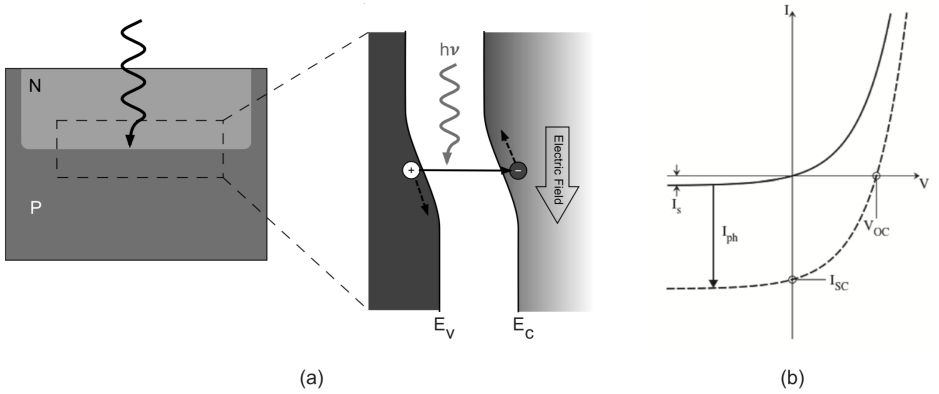

FIGURE 2.6: Photogeneration in a PN junction. (Source: [13])

Fig.2.5(c) the resulting net charge density distribution, Fig.2.5(d) the resulting electric field and Fig.2.5(e) the band diagram of a typical PN junction showing the the shifting and alignment of the bands. Without external electric field, a PN junction has a built-in electric field by nature due to the charge distribution shown in 2.5(c), which is a state of equilibrium from the diffusion, drift and recombination processes. The built-in electric field also results in a potential difference of V_0 between the two sides[13].

When a photon hits the depletion region as shown in Fig.2.6(a), an electron-hole pair is generated. Because of the built-in electric field mentioned before, the generated carriers are pushed away from the depletion region, with the electron drifting towards the n-side and the hole towards the p-side. This movement of charges produces an electric current called the photocurrent flowing from the n-side to the p-side, which shifts the $I - V$ graph of the diode downwards by amount of I_{ph} equal to the photocurrent. With the Schottky Equation for ideal $I - V$ characteristics of diodes[9], the shifted curve shown in Fig.2.6(b) can be expressed as follows[13]:

$$I = I_S[e^{qV/kT} - 1] - I_{ph} \tag{2.10}$$

where I_S is the saturation current, k the Boltzmann constant and T the operation temperature.

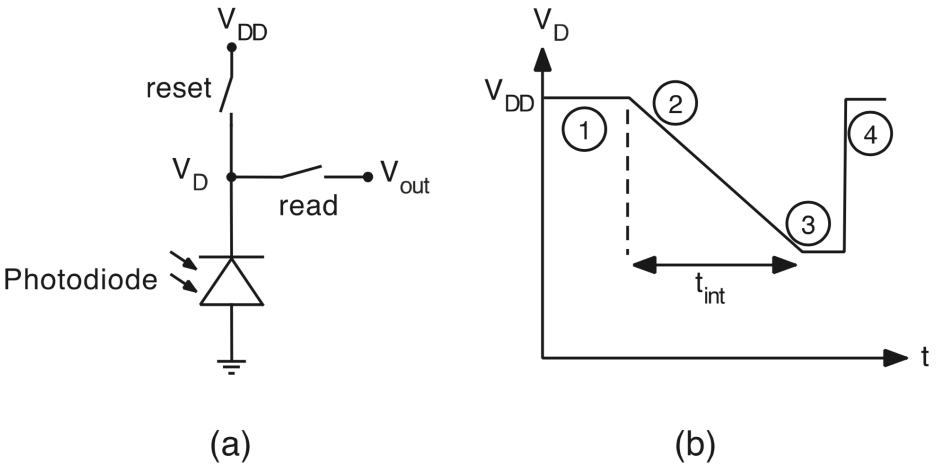

FIGURE 2.7: Abstract circuit for accumulation mode operation. (Source: [13])

Accumulation Mode

Photodiodes working in accumulation mode are used in CCD and CMOS imaging. This is because accumulation mode allows charge to accumulate so that stronger integrated signals that more faithfully represent the light intensity are produced[13]. The charge accumulation can be achieved using the abstract circuit shown in Fig.2.7(a) for a pixel in an imaging array and an operation cycle shown in Fig.2.7(b). Here is a brief description of the operation cycle[13]:

① At first, the reset switch is closed to set $V_D = V_{DD}$. The photodiode is in reverse bias.

② After the reset switch opens, the process of photon collection begins and the photocurrent starts to drain the charges. V_D drops.

③ After an integration time t_{int}, we stop the photon collection and close the read switch to get $V_{out} = V_D$.

④ Finally, the read switch opens and the reset switch is closed again. Repeat from the first step.

This operation circle can be repeated continuously and we can get a measurement of the light intensity based on the voltage drop $V_{DD} - V_{out}$ at each pixel.

P-i-N Photodiodes

Adding an intrinsic region between the p- and n-type regions can increase the active region for carrier generation, which increases the photon collection efficiency. Fig.2.8 shows the properties of ideal P-i-N junctions under reverse bias. Fig.2.8(a) gives the structure of a P-i-N junction, Fig.2.8(b) the resulting

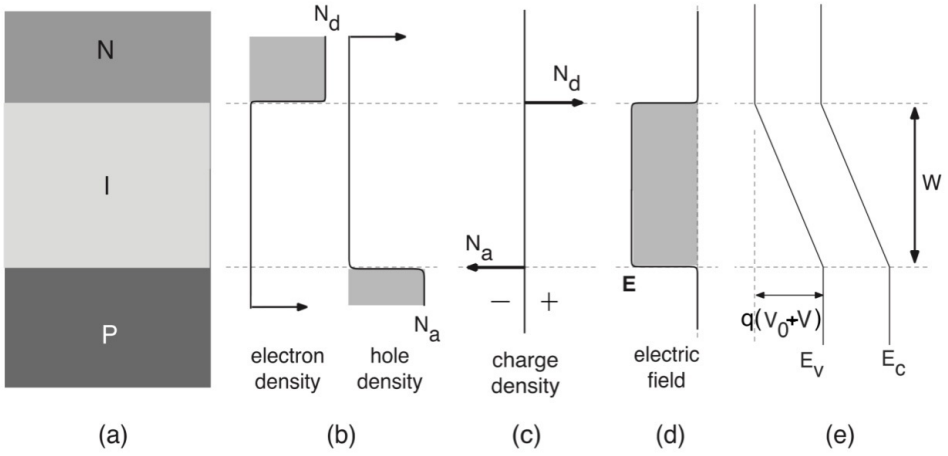

FIGURE 2.8: Ideal P-i-N junction properties. (Source: [13])

electron and hole density distribution, Fig.2.8(c) the resulting net charge density distribution, Fig.2.8(d) the resulting electric field and Fig.2.8(e) the band diagram. Note there are two assumptions underlying Fig.2.8: (1) there is no net charge in the intrinsic region because the external reverse electric field has driven all the carriers away; and (2) two depletion regions formed on the two sides of the doped-intrinsic junction are very narrow[8]. The resulting electric field E in the intrinsic region is

$$E = \frac{V_0 + V}{W} \tag{2.11}$$

where V_0 is the built-in potential, and V is the amplitude of the reverse bias voltage.

2.3.2 Pinned Photodiodes (PPD)

Pinned photodiode (PPD) was originally invented in 1982 to reduce the image lag in CCD sensors. This new structure added a p^+ layer on top of the n-layer of a normal photodiode, which effectively suppresses the surface generated dark current. The cross-section of a PPD is shown in Fig.2.9.

When implemented as pixel as shown in Fig.2.10, PPD is controlled by a transfer gate (TG): during light integration, TG is set to off so that the PPD is isolated from the floating diffusion node (FD); after light integration, TG is enabled to transfer electrons from PPD to FD. This basic operation is demonstrated in Fig.2.11.

PPD has a structure in which the sense node is separated from its integration node, and thus kTC noise can be removed by sampling methods. However, PPDs have smaller fill factor compared with photodiodes.

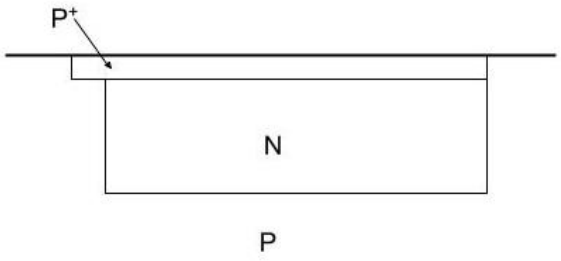

FIGURE 2.9: Cross-section of PPD.

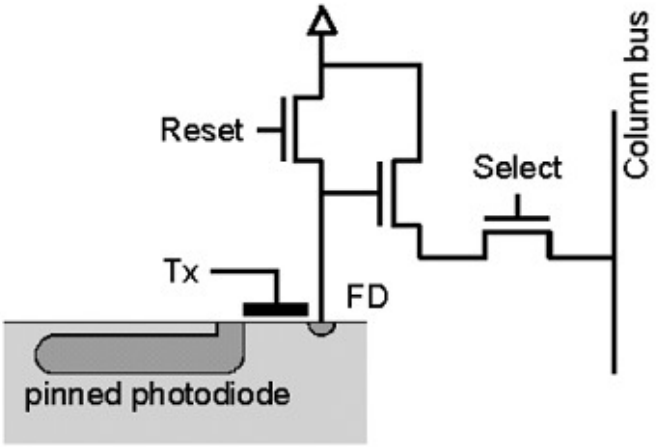

FIGURE 2.10: PPD pixel. (Source: [1])

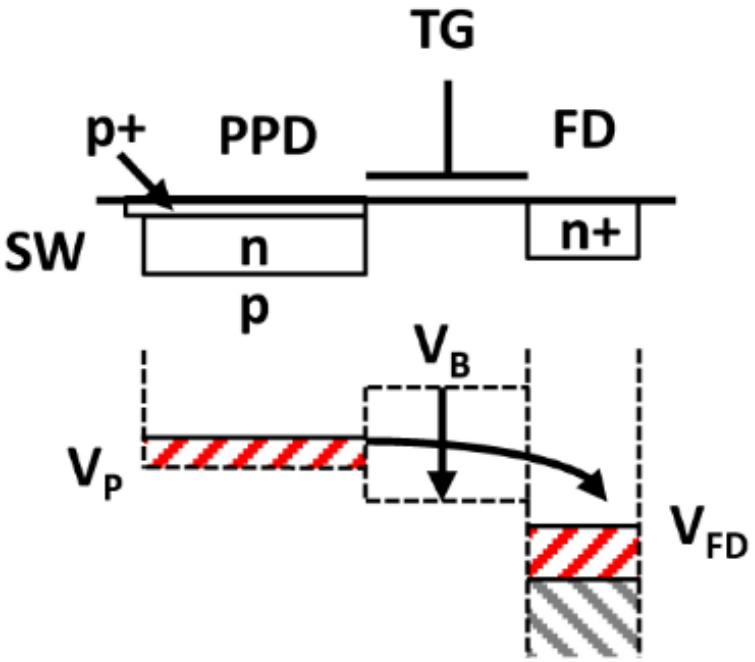

FIGURE 2.11: PPD basic operation. (Source: [1])

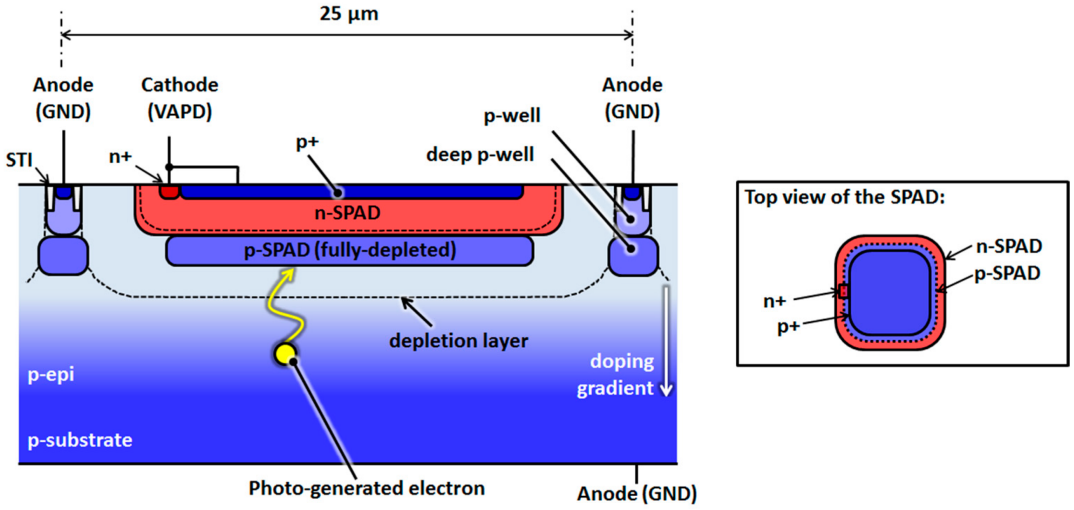

FIGURE 2.12: SPAD structure. (Source: [13])

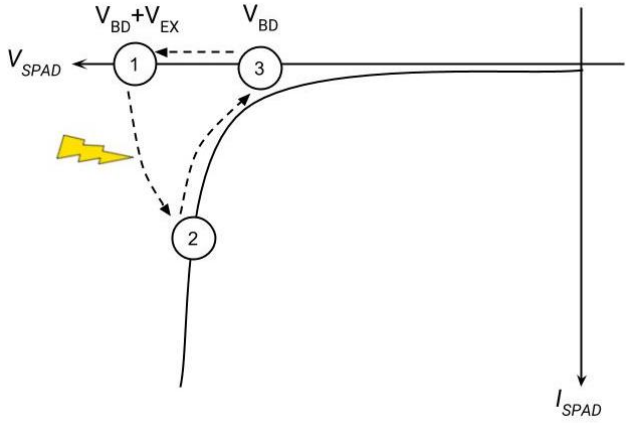

FIGURE 2.13: SPAD operation cycle.

2.3.3 Single-Photon Avalanche Diodes (SPADs)

Single-photon avalanche diode (SPAD) is a PN junction that operates at a reverse biased voltage above the breakdown voltage, where a single photo-generated carrier can trigger an avalanche current. The cross-section and top view of the SPAD is shown in Fig.2.12.

The basic operation mode is shown in Fig.2.13, where V_{BD} is the breakdown voltage and $V_{BD} + V_{EX}$ is the operation voltage. Charged to a voltage higher than the breakdown voltage, the SPAD is initially in a metastable state at ①. The state can be perturbed by the arrival of a photon, which triggers an avalanche and pushes the state to ②. Between ② and ③ is a quenching period where outside device counteracts the current by decreasing the voltage across the SPAD. Finally, the diode can be again recharged to operation voltage.

SPAD Specific Performance Metrics

- **Dark Count Rate (DCR)**: the frequency of occurrence of avalanches when there is no light. DCR represents the base noise level. It is measured in hertz and depends on the excess bias and temperature.
- **Photon Detection Probability (PDP)**: the probability that an photon incident onto the SPAD's active area triggers an avalanche.
- **Dead Time**: the time for a SPAD to get ready for another avalanche.

2.3.4 Photogates (MOS Capacitors)

Photogate, also known as MOS capacitor, is a type of semiconductor devices widely used in the CMOS and CCD image sensors. Its structure is shown in Fig.2.14.

When used as photodetectors, photogates usually operates in the deep depletion regime where the metal layer is connected to a gate voltage v_G that is far greater than the threshold voltage. Electrons generated in the depletion region are collected in the potential well.

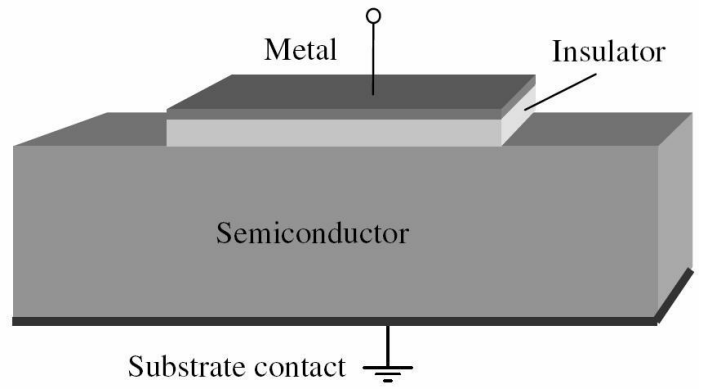

FIGURE 2.14: Photogate structure. (Source: [8])

2.4 Conventional Sensor Technologies Revisited

2.4.1 CCD Image Sensors

CCD consists of a series of photogates mentioned in Section 2.3.4. They are coupled with one another. The charges are stored in the potential well and are shifted from one gate to the next in the CCD circuit by fringing electric field, potential and carrier density gradient.

The charges can be shifted from one gate to adjacent one by manipulating the gate voltages, as shown in Fig.2.15.

To transfer charges in CCDs, a uni-directional potential gradient should be provided along a linear array of CCD's. The number of different voltages applied to the electrodes determines how many phases the clocking should

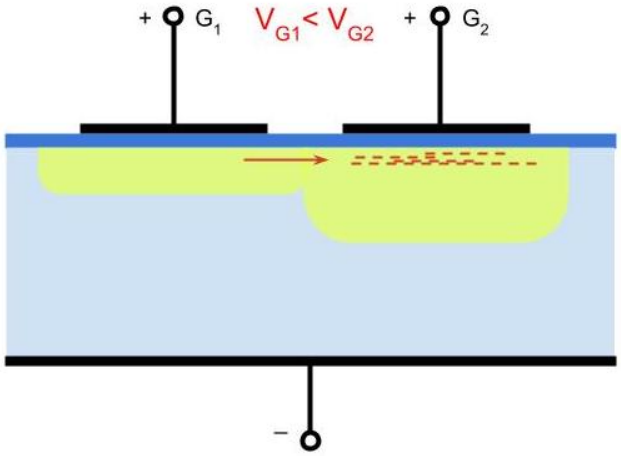

FIGURE 2.15: Charge transfer between gates.

have. As an example, the charge transfer scheme in a 3-phase CCD is shown in Fig.2.16.

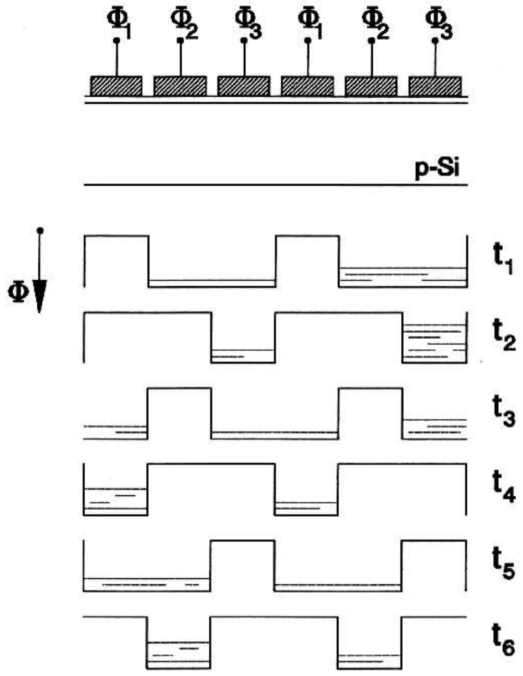

FIGURE 2.16: Charge transfer in 3-phase CCD. (Source: [12])

To make s 2D CCD image sensor, the 1D CCD imaging arrays are put parallel to each other as adjacent columns that are coupled into a horizontal CCD shift register to combine their outputs into a row-by-row serial bit stream of the image. Each pixel value is read serially through the floating diffusion node in the end. The structure of a typical frame transfer (FT) CCD is shown in Fig.2.1.

Pros and Cons

CCD image sensors have the following advantages[4]:

- Relatively high fill factor.
- Low noise.
- High sensitivity (QE$\approx$ 80%.)

However, the major limitations of CCD technology are[7]:

- High power consumption because of high-speed clocks and high operating voltage.
- Limited frame rate and processing speed due to the slow serial readout (less than 20fps.)
- Incompatibility with most analog or digital circuits.
- Requirement of a specialized fabrication process.
- Blooming and smearing due to overexposure.

2.4.2 CMOS Image Sensors

CMOS pixel sensor uses photodiodes for photodetection. Unlike CCDs, CMOS imager offers access to individual pixel directly. As shown in Fig.2.2, for CMOS pixels the in-pixel processing converts the photo-generated charge to a voltage and then outputs the voltage directly. The pixel value can be read out using the column decoder and multiplexer similar to those in DRAM memories.

There are two types of CMOS pixel sensor – passive pixel sensor (PPS) and active pixel sensor (APS) – depending on whether each pixel has its own amplifier and active noise canceling circuitry. Passive pixel sensors do not have the built-in amplifiers, and there is only one transistor per pixel. They are very slow and noisy. However, active pixel sensors are fast with higher SNR than passive pixel sensors, and they are the current technology of choice. The architecture of an active pixel sensor is shown in Fig.2.17.

Pros and Cons

CMOS image sensors are becoming more and more popular in digiral photography in recent years. They have the following advantages[11]:

- High frame rate and fast readout.
- Low power consumption and low voltage operation.
- Fabricated using standard CMOS process.
- Random accessibility of individual pixels.

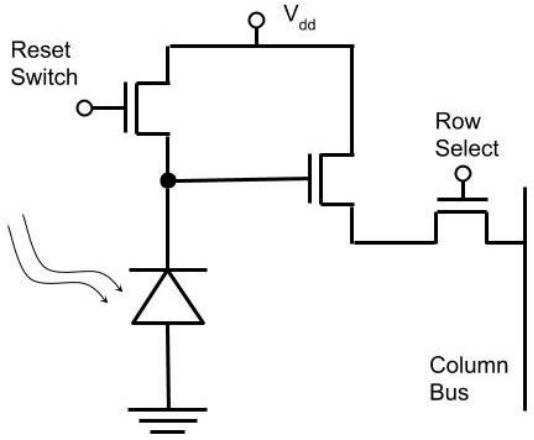

FIGURE 2.17: Active Pixel Sensor (APS)

- Good performance in brightly lit situations.

The major limitations of CMOS technology are[4]:

- Relatively higher noise level and patterned noise.
- Low fill factor due to in-pixel processing.

2.4.3 Dynamic range: fixed frame time

Both CCD and CMOS image sensors rely on framed capture: all pixels are illuminated using a shutter for a fixed time interval. This fixed frame time not only forces synchronicity on all pixels, but also limits dynamic range because bright pixels and dark pixels do not have the freedom to use different frame time. When there is a broad range of luminance present in the environment, conventional cameras fail to capture the whole range because either bright pixels overflow, or dark ones underflow.

This limitation in dynamic range originates from how the light intensity is measured in CCD and CMOS image sensors. The ratio of the number of photons accumulated in each pixel to the frame time is a measure of the light intensity, and when the frame time is fixed for one picture, the dynamic range thus is limited by the "photon capacity" of one pixel, which is technically called full well capacity.

2.4.4 Summary

Table 2.1 summarizes some of the characteristics of CCD and CMOS image sensors. In general, CCD imagers are better for low-light operation because of their low noise floors, and are the preferred technology in astronomy; while CMOS image sensors are becoming increasingly popular in recent years for general purpose photography because of their lower cost and power consumption. However, with fixed acquisition time for all pixels in one frame, the dynamic range for both technologies are limited by the pixel sensitivity and full well capacity.

Technology	CCD	CMOS
Frame rate	Moderate	Fast
Noise	Low	Moderate
Fill factor	High	Low
Power consumption	High	Low
Costs for manufacture	High	Low
Pixel accessibility	No	Yes
Voltage levels needed	Many	Few
Image quality: low-light condition	Good	Moderate to good
Image quality: brightly-lit condition	Blooming/smearing	Good

TABLE 2.1: Summary of CCD and CMOS image sensors.

Chapter 3

Background: Frameless Image Sensor

A system model of frameless asynchronous sensors is proposed by Singh et al. in [10]. Unlike conventional CCD and CMOS image sensors that estimate the number of photons each pixel accumulates in a fixed amount of time, this new design utilizes an alternative approach that measures the integration time for each pixel to accumulate a fixed number of photons. Following the discussion in Section 2.4.3 that the light intensity at each pixel is determined by the ratio of the number of arrival photons to the accumulation time. If the number of photons is fixed, the light intensity becomes inversely proportional to the integration time that can vary from $1ns$ to infinity. In this way, the darker pixels take longer to accumulate photons and the brighter ones take less; therefore, the dynamic range is no longer limited by the pixel sensitivity and full well capacitor.

3.1 Design

The architecture of a frameless pixel is given in Fig.3.1. Unlike conventional CMOS sensors, frameless pixel has an integrated comparator that resets the photodiode when the photons are accumulated to a threshold value, which results in a spike in the output voltage. The circuit implementation for a frameless pixel is shown in Fig.3.2. And sample diagram of the voltage V_D and V_{out} as a function of time with varying light intensity is given in Fig.3.3.

The prescaler/decimator is a simple frequency divider that transmits one spike event to the column readout for every 2^D spikes; thus, it avoids sending too many events to the column. If the time interval between spike events

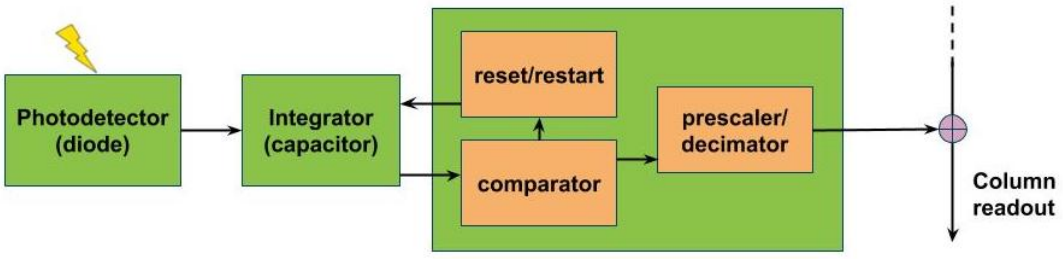

FIGURE 3.1: Frameless pixel architecture (Follow [10])

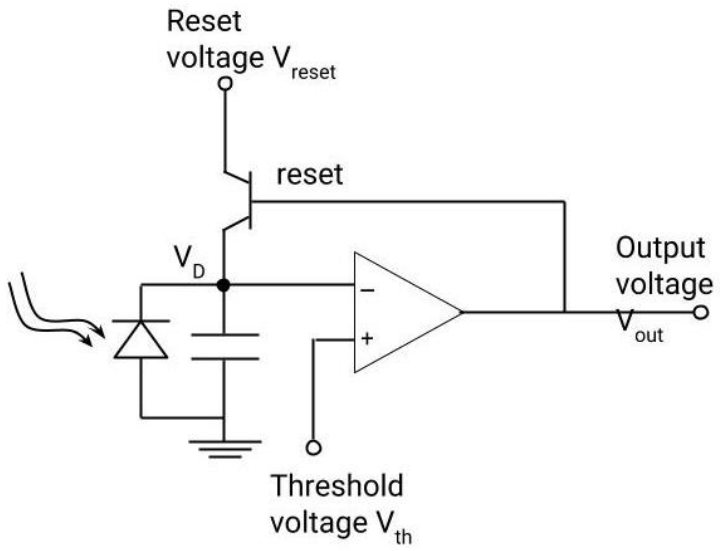

FIGURE 3.2: Frameless pixel circuit implementation

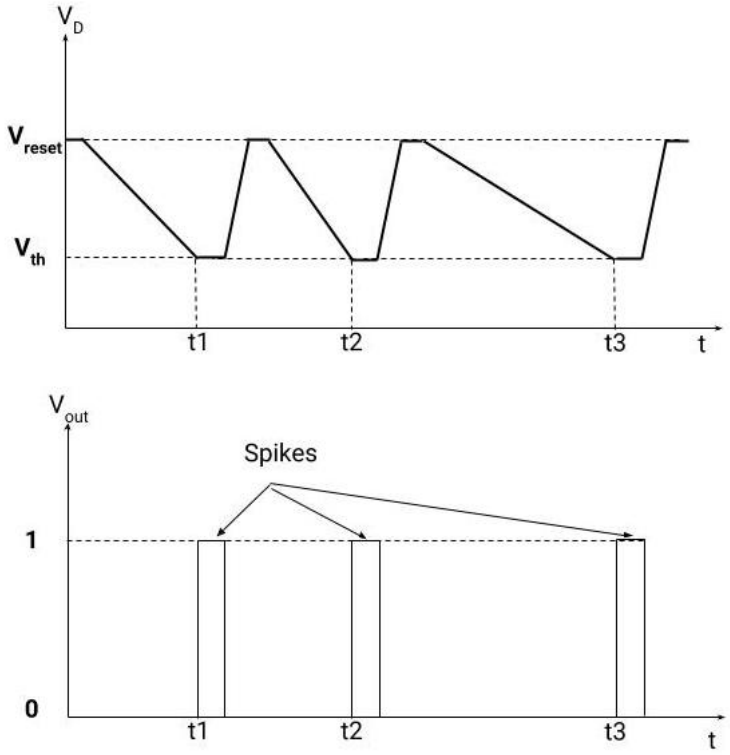

FIGURE 3.3: Example V_D and V_{out} waveform.

from column is ΔT:

$$\text{light intensity} \propto \frac{2^D}{\Delta T}. \tag{3.1}$$

3.2 Advantages

The frameless design will have the following benefits over those traditional framed capture architectures [10]:

- **Frameless capture**: each pixel's saturation time is independently measured.
- **Wider dynamic range**: More time for accumulating photons means longer exposure time.
- **Greater precision**: Time measurement is much more precise than photon accumulation, yielding intensity values with precision of 20 bits.
- **Bandwidth allocation**: The configurable saturation threshold for each pixel allows the sensor to increase sensitivity in particular regions of interest.

Chapter 4

Improvement 1: Low-Light Detection via Noise Reduction

4.1 Challenge: Noise

In low light regime, noise overwhelms the small low-light signal. The noise floor limits the camera performance because signal measurements less than noise floor are unreliable. However, many astronomy applications ask for cameras that are able to work in that "noisy zone". Therefore, decreasing the noise level is the critical step to improve the camera performance, even for the frameless sensor. The limiting factor for low-light pixel performance is the kTC reset noise.

4.1.1 kTC Reset Noise

The reset noise, also known as kTC noise, is the noise introduced when resetting the capacitor. The purpose of a reset operation is to provide a reference level for comparison with the number of electrons generated from photons incident to the photodiode. The reset noise originates from the thermal noise that causes voltage fluctuations in the reset level. As a result, the reset voltage is a random variable that has a mean equal to V_{reset} and a standard deviation equal to the reset noise $\sqrt{kT/C}$. Here, T is the temperature, k is Boltzmann constant, and C is the capacitance. A noisy reset operation undermines the pixel performance especially in low light level conditions because of an increased noise floor. The misplacement of a single electron can typically generate $50\mu V$ of noise across a capacitance of 3fF[2]. This is a significant change in voltage compared to the generated signal and a major problem for most CMOS-based sensors.

4.2 Approaches to Mitigate Reset Noise

4.2.1 Noise subtraction via two-threshold sampling

The reset noise can be subtracted by setting a second threshold that is below the lower bound of the reset voltage but higher than the original one. The diagram of the circuit implementation is given in Fig.4.1, where the two comparators are used for the two thresholds respectively. When the value

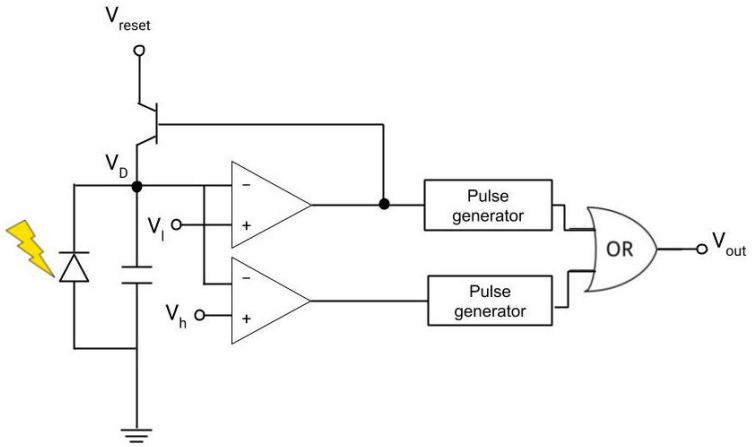

FIGURE 4.1: Circuit implementation of the two-threshold sampling.

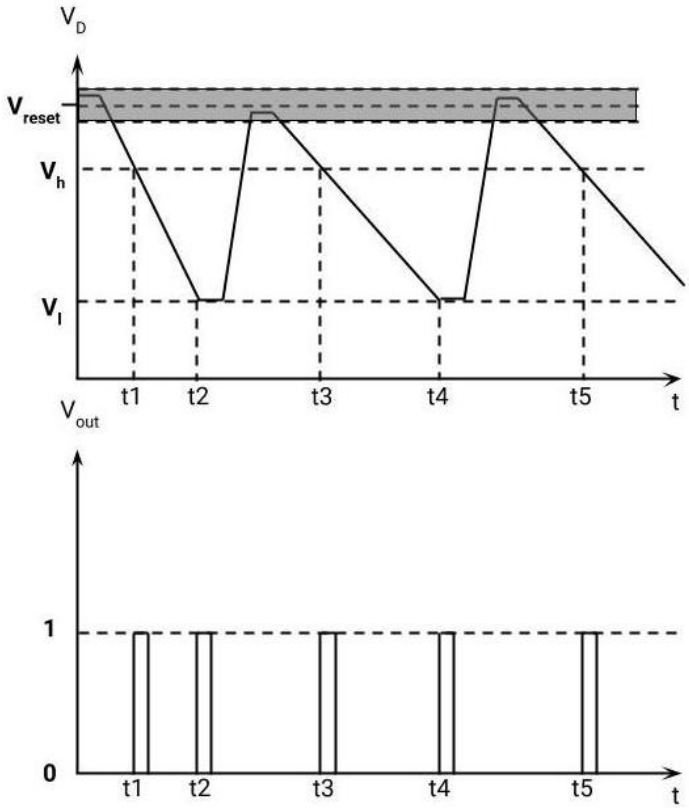

FIGURE 4.2: Example V_D and V_{out} waveforms with two-threshold sampling

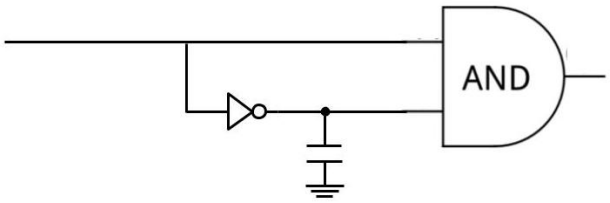

FIGURE 4.3: Circuit implementation of a pulse generator.

of V_D drops to cross either of the threshold values (i,e. V_h/V_l), the output of the corresponding comparator changes from 0 to 1. The pulse generators convert the comparator outputs to spikes when the signals change from 0 to 1. Finally, the OR gate combines the spikes from the two pulse generators and outputs the combined signal.

The two thresholds will produce two spikes on the output for a single operation cycle. The two spikes can be tagged with a single bit to distinguish between signals from threshold V_l or V_h. An example graph of how V_D and V_{out} change over time is shown in Fig.4.2. The intensity can now be correctly calculated from the two known crossing points.

There are two regimes of operation. Under low light regime, the prescaler is typically not used because the frequency of pulses is low; therefore, both spikes from one operation cycle get through to the column pipeline. The processing logic will then subtract the time stamps of the two spikes. Under high light regime, the prescaler will always get rid of the first threshold crossing because the frequency of pulses is high. The whole operation effectively reverts to the original operation when there is only one single threshold. Since many spikes are generated, the reset noise is automatically averaged.

The pulse generator can be implemented using the circuit diagram given in Fig.4.3, where the capacitance of the capacitor can be adjusted to set the width of spikes.

4.2.2 Noise averaging via repeated sampling

Because the reset noise is random noise by nature, it averaged out when the sample size is large. Therefore, speeding up the spike events together with using the prescaler for averaging can effectively reduce the reset noise by increasing the sample size.

To raise the baseline spike frequency, a known current source in parallel to the photodiode can be added to the circuit. The circuit implementation is given in Fig.4.4. The known current source adds a constant current offset to the photocurrent so that the capacitor is drained more quickly. The actual spiking frequency caused by the incident light can be recovered by subtracting a base frequency caused by the known current. Two graphs showing the voltage V_D before and after implementing the current source is shown in Fig.4.5. We can see an increase in the number of spike events.

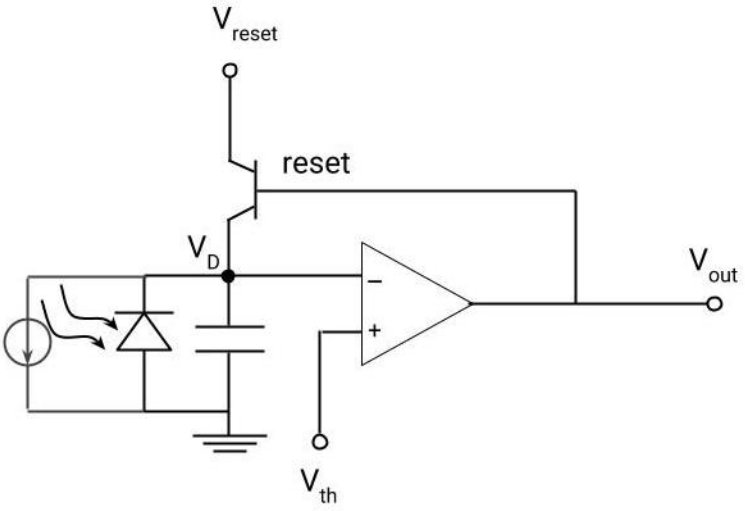

FIGURE 4.4: Circuit implementation of the repeated sampling.

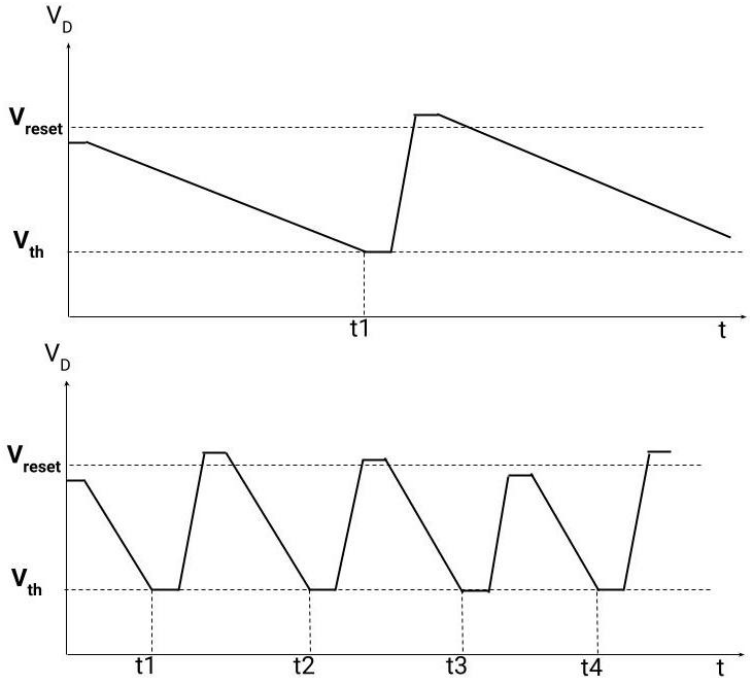

FIGURE 4.5: Example V_D and V_{out} waveforms before/after applying two-threshold sampling. (Upper: before. Lower: after)

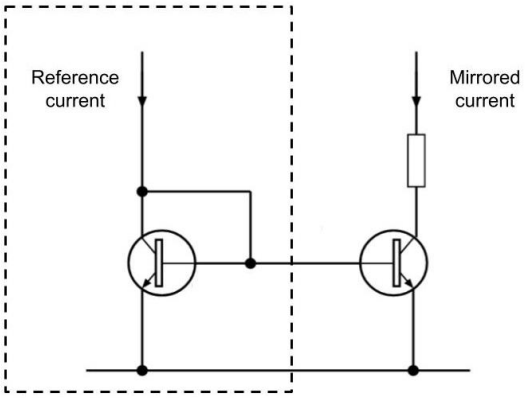

FIGURE 4.6: Simple current mirror circuit.

The current source is a well known analog circuit. we can match every pixel current with one reference current throughout the sensor chip using the current mirror circuit shown in Fig4.6. The circuit circled by dotted line is common to every pixel and is placed off pixel array.

4.2.3 Combined approach

The problem of using the two-threshold sampling alone for low-light environment is that some pixels can be too dark to provide spikes that are temporally meaningful, that is, failing to capture immediate information. When the two-threshold and repeated sampling methods are combined, the major benefit of this combined approach is the increase in the spike frequency for two-threshold sampling even under extreme low-light conditions. The circuit implementation is given in Fig.4.7.

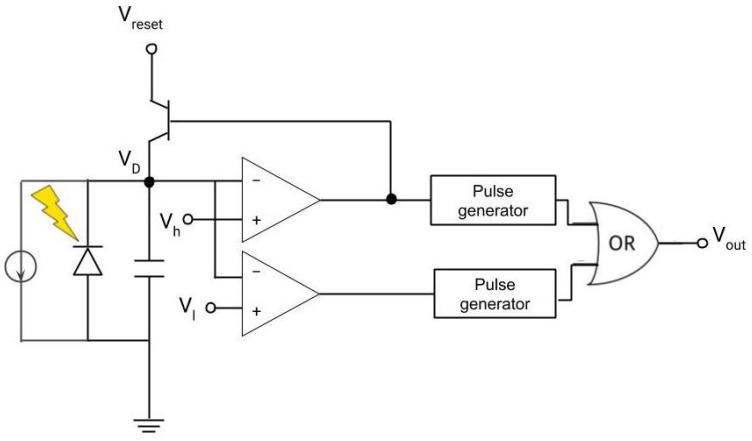

FIGURE 4.7: Circuit implementation of the combined approach.

4.3 Summary

In this Chapter, we explore the noise challenge of camera's low-light operation, and specifically focus on the reset noise, which is the limiting factor for pixel performance. Three approaches to reduce the reset noise are proposed: two-threshold sampling that subtracts the reset noise, repeated sampling that averages the reset noise, and the combined approach of the previous two methods.

Chapter 5

Improvement 2: Single Photon Detection

5.1 Single-Photon Avalanche Diode (SPAD) Implementation

As introduced in Section 2.3.3, SPADs can detect the arrival of a single photon. Such single photon sensing is beneficial for imaging in astronomy because the targets are so faint that from them each pixel can only collects dozens of photons. By implementing SPADs into the frameless camera architecture, we can identify the timestamp of the arrival of individual photons based on the spikes, and obtain valuable time series information on those stars from which the photons came.

5.1.1 Circuit Design

To make possible the single photon detection, the implementation of SPAD also requires an accompanying quenching circuit that distinguishes the avalanche. It can be divided into two categories: passive quenching and active quenching. The passive quenching scheme is composed of a simple resistor or properly biased transistor that slowly drains the avalanche current until the avalanche is turned off. Then, within the resistance-capacitance time constant of the circuit, the device is recharged to the full voltage.

Active quenching, on the other hand, is triggered by some electronics that sense the occurrence of an avalanche and turning off the SPAD immediately. The device is recharged for the next detection more quickly than passive quenching, reducing the dead time. It also suppresses the overall amount of avalanche current and therefore decreasing the afterpulsing probability, which is the probability of additional correlated avalanches caused by the charges trapped inside deep levels rather than photo-generated charges.

The frameless pixel circuit implementation in Fig.3.2 can be adapted for active quenching because the camparator is perfect for sensing the avalanche. The circuit implementation for single photon detection is shown in Fig.5.1, where V_{off} is the voltage for quenching the avalanche and the pulse generator producing a short pulse every time when the comparator's output changes from 0 to 1. V_{off} should be high enough to decrease the voltage

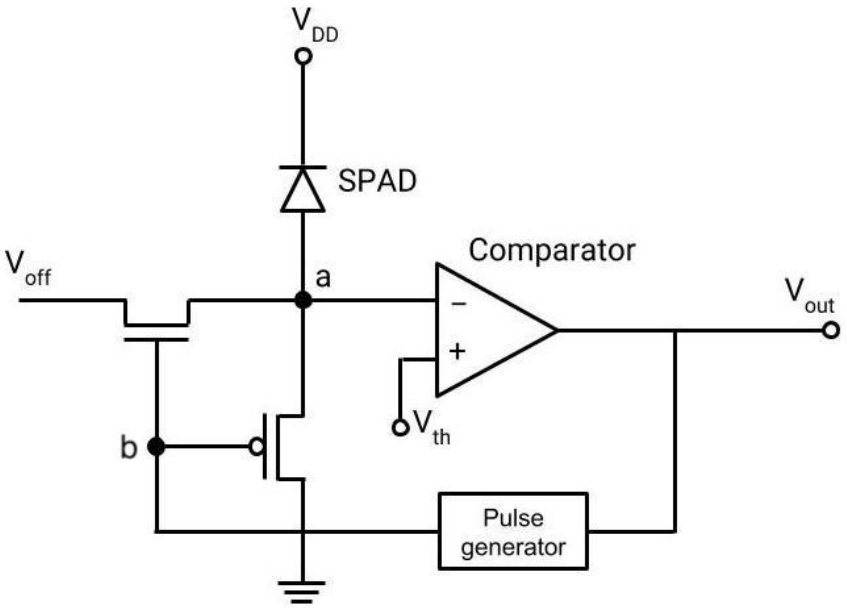

FIGURE 5.1: Circuit implementation for single photon detection using SPAD.

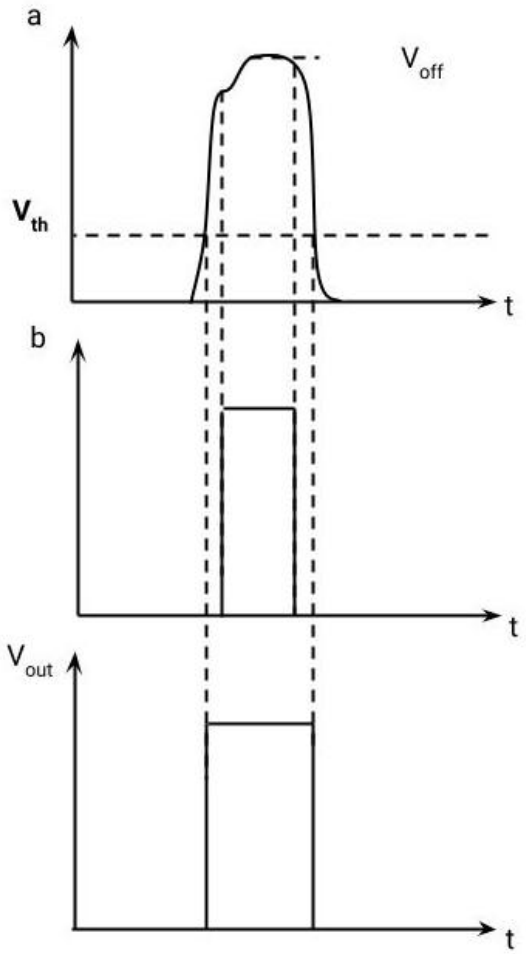

FIGURE 5.2: The voltages at *a*, *b* and output after the occurrence of a single photon.

across the SPAD so that avalanche is effectively distinguished. The pulse generator can be implemented using the same circuit shown in Fig.2.3.4.

Fig.5.2 shows how the voltages at a, b, and the output change after the occurrence of a single photon. The voltage at point a is the anode voltage of SPAD, while the SPAD's cathode is held constant at V_{DD}. Point b is connected directly to the output of pulse generator, and the width of the pulse can be set by adjusting the capacitance inside the pulse generator. V_{out} is the output of the comparator. Between the comparator's output switching to 1 and the pulse generator producing a pulse, there is a small time delay and it is exaggerated in Fig.5.2.

We can see after the avalanche begins but before the left transistor is turned on, the voltage at point a rises rapidly from zero. This is when the avalanche occurs. Then, when left transistor is turned on, the voltage at point a is set to V_{off}, which decreases the voltage across the SPAD to a value below the breakdown voltage and turns off the avalanche immediately. After an active quenching time determined by the pulse generator, the voltage at point b is low again so that the left transistor is turned off but the transistor connected to the ground is turned on. This time, the voltage at point a is lowered to zero which quickly recharged the SPAD. After V_{out} is low again, the pixel is ready for another detection.

5.1.2 Challenges

Single photon detection can be a powerful feature for frameless image sensors, but the implementation of SPAD also raises many challenges.

- The photon detection probability (PDP) is limited even in visible spectrum.
- The dark count rate (DCR) grows exponentially with temperature, which requires a low operating temperature down to -40°C to get a DCR less than 10.
- Applying a higher voltage improves PDP, but also increases the DCR.
- The dead time limits the time resolution because an immediate photon arrives within the dead time cannot be detected.

Chapter 6

Summary and Conclusion

In this work, we reviewed the basics of image sensors and conventional CCD and CMOS imaging technologies. Built upon a frameless camera architecture proposed in [10], we introduced several enhancements to the frameless sensor design to improve its low-light performance. Specifically, three methods for noise reduction are introduced: the two-threshold sampling that subtracts the noise, the repeated sampling that averages the noise, and a combined approach for extremely low-light imaging. We also introduce the single photon detection by implementing the single-photon avalanche diode to detect the arrival of a single photon. These improvements aim at improving the performance of the frameless image sensor under the low-light condition typical for astronomy.

6.1 Comparison

Table 6.1 shows a comparison among conventional CCD and CMOS sensors and our new frameless image sensors with or without the noise reduction or the single photon detection functionality that I introduced. The low-light sensitivity, the performance under bright domain, the dynamic range, the reset noise (noise floor), and the availability of time-series information and pixel accessibility are compared. We can see the frameless image sensor not only greatly improves the dynamic range and thus the bright-domain operation, but also makes the time-series information available. However, frameless imaging with single photon detection presumably does not suit the operation in brightly-lit environment because the frequency of the pixel signals can easily reach the upper bound due to the overwhelming photons, which makes bright pixels indistinguishable. On the other hand, photons arriving at the same time can only be counted once, resulting in the loss of precision. But the introduction of single photon detection frees the camera sensor from reset noise, and makes each pixel sensitive to a single photon, suitable for operations in low-light environment.

Like conventional CMOS-based image sensor, the frameless image sensor also inherits the pixel accessibility. However, the pixel-level analog-to-digital signal conversion also introduces the high reset noise at the same time. This problem is addressed by our noise reduction techniques that subtract and average the noise. By reducing the reset noise that determines the noise floor, we improve the sensor's low-light sensitivity.

	CCD	CMOS	Frameless	Frameless +noise reduction	Frameless +single photon detection
Dynamic range	Blooming smearing	Moderate	Good	Good	Good
Bright domain	Blooming smearing	Moderate	Good	Good	Not suitable
Reset noise	Low	High	High	Low	Not a concern
Low-light sensitivity	Good	Limited	Limited	Improved	Sensitive to a single photon
Pixel accessibility	No	Yes	Yes	Yes	Yes
Time-series information	No	No	Yes	Yes	Yes

TABLE 6.1: Comparison among CCD, CMOS, frameless, frameless with noise reduction, and frameless with single photon detection image sensors.

6.2 Future work

Future work should first focus on the circuit simulation to check the integrity of the circuit design. Specifically, the noise level for the frameless pixels using different noise-reduction methods should be checked and optimized. For single photon detection, the trade-offs between the key parameters of SPADs and the dark count rate should be studied during simulation for further optimization. All the simulation should consider different lighting conditions and light spectra of interest.

After simulation, we can look for chip-level complete circuit implementation to deal with problems that are missed or do not occur during simulation, and evaluate the design in an actual camera setup.

Bibliography

1. <http://webee.technion.ac.il/labs/vlsi/Projects/PR210/eeigor_APS_e.files/> (2012).
2. Calizo, I. G. Reset noise in CMOS image sensors (2005).
3. Clark, R. N. *Digital Camera Reviews and Sensor Performance Summary* (Oct. 2016). <http://www.clarkvision.com/articles/digital.sensor.performance.summary>.
4. El Gamal, A. *Introduction to Image Sensors an Digital Cameras* Apr. 2001.
5. Fellers, T. J. & Davidson, M. W. *CCD Noise Sources and Signal-to-Noise Ratio* (). <http://hamamatsu.magnet.fsu.edu/articles/ccdsnr.html>.
6. Fellers, T. J. & Davidson, M. W. *Digital Camera Readout and Frame Rates* (). <http://hamamatsu.magnet.fsu.edu/articles/readoutandframerates.html>.
7. Fossum, E. R. Active pixel sensors: are CCDs dinosaurs? **1900.** doi:10.1117/12.148585. <https://doi.org/10.1117/12.148585> (1993).
8. Sapoval, B. & Hermann, C. *Physics of semiconductors* ISBN: 9780387940243. <https://books.google.com/books?id=P6wPAQAAMAAJ> (Springer-Verlag, 1995).
9. Shockley, W. The theory of p-n junctions in semiconductors and p-n junction transistors. *The Bell System Technical Journal* **28,** 435–489. ISSN: 0005-8580 (July 1949).
10. Singh, M., Zhang, P., Vitkus, A., Mayer-Patel, K. & Vicci, L. *A Frameless Imaging Sensor with Asynchronous Pixels: An Architectural Evaluation* in *2017 23rd IEEE International Symposium on Asynchronous Circuits and Systems (ASYNC)* (May 2017), 110–117. doi:10.1109/ASYNC.2017.19.
11. Tabet, M. Double sampling techniques for CMOS Image Sensors (Jan. 2002).
12. Theuwissen, A. *Solid-State Imaging with Charge-Coupled Devices* ISBN: 9780792334569. <https://books.google.com/books?id=dchEKTHNCMcC> (Springer Netherlands, 1995).
13. Titus, A., Cheung, M. & P. Chodavarapu, V. in, 65–102 (July 2011). ISBN: 978-953-307-530-3. doi:10.5772/20194.